

ANTNets: Mobile Convolutional Neural Networks for Resource Efficient Image Classification

Yunyang Xiong*
University of Wisconsin-Madison
yxiong43@wisc.edu

Hyunwoo J. Kim*
Korea University
hyunwoojkim@korea.ac.kr

Varsha Hedau
Amazon Inc.
hedauv@amazon.com

Abstract

Deep convolutional neural networks have achieved remarkable success in computer vision. However, deep neural networks require large computing resources to achieve high performance. Although depthwise separable convolution can be an efficient module to approximate a standard convolution, it often leads to reduced representational power of networks. In this paper, under budget constraints such as computational cost (MAdds) and the parameter count, we propose a novel basic architectural block, ANTBlock. It boosts the representational power by modeling, in a high dimensional space, interdependency of channels between a depthwise convolution layer and a projection layer in the ANTBlocks. Our experiments show that ANTNet built by a sequence of ANTBlocks, consistently outperforms state-of-the-art low-cost mobile convolutional neural networks across multiple datasets. On CIFAR100, our model achieves 75.7% top-1 accuracy, which is 1.5% higher than MobileNetV2 with 8.3% fewer parameters and 19.6% less computational cost. On ImageNet, our model achieves 72.8% top-1 accuracy, which is 0.8% improvement, with 157.7ms (20% faster) on iPhone 5s over MobileNetV2.

1. Introduction

Deep neural networks have emerged as state-of-the-art solutions for various tasks in computer vision, machine learning, and natural language processing. Recent research in deep learning mainly focuses on deeper and heavier models to achieve superhuman accuracy with a tremendous number of parameters. Inception [12], ResNets [5], HighwayNets [22], and DenseNet [10] are popular architectures in this direction and has been shown to be effective in a variety of tasks. However, in many real-world applications, due to limited computing resources and short latency requirements, more efficient recognition systems are often required, for example, in mobile phones, robots, and smart

appliances that require the on-device intelligence systems.

For the last few years, small and efficient neural networks have enabled the deployment of models on computationally limited hardware for a wide range of applications. One stream of such efforts is to substitute existing layers with more efficient layers. Since in a vision system, convolutional neural networks (CNNs) are the most popular base feature extraction networks and the main computational burden is convolutional layers, faster convolution layers are crucial. The standard convolution layer performs convolution using all the input channels for one output channel. So, the number of filters and calculations increase as the number of input channels grows. Instead, *group convolution* involves only each group of input channels resulting in a smaller number of filters (and calculations) reduced by a factor of the number of groups. Group convolution has been used in multiple architectures. AlexNet [15] uses group convolution to train models on GPUs with limited memory. Later, ResNeXt [25] utilizes group convolution to achieve better performance and [11] proposed more complex group convolution with hierarchical arrangements. One extreme of group convolution is *depthwise separable convolutions* introduced in [21]. Each group involves only one input channel and convolution filter. Since then, the trick has been adopted in other architectures such as Inception [12], Flattened Networks [13] and Xception [2]. Recently, the depthwise separable convolution has been adopted by a compact architecture specifically designed for mobile devices. MobileNetV1 [6], and MobileNetV2 [20] achieved significant improvement with respect to inference time (latency) on mobile devices.

Efficient convolutional layers are preferable but accuracy degradation is inevitable. To fill the performance gap induced by approximate convolution, recent network enhancement techniques can be used as long as the additional cost is negligible. There have been multiple attempts to boost the representational power of models with negligible additional cost. Attentional neural networks have been proven that it is a general module and improve performance by suppressing irrelevant information and focus on informa-

*Work done at Amazon Lab126.

tive parts of data. Temporal/spatial attention has been studied in the literature but, arguably, they come with a significant cost. However, channel attention can be implemented in a much more efficient way. For instance, the ‘‘Squeeze-and-Excitation’’ (SE) block proposed in SENet [8] allows selective reweighting channels based on global information from each channel. This improves a variety of architectures with a minor computational cost. A channel shuffle operation also boosts the performance or mitigates degradation of group convolution as shown in ShuffleNet [27, 18] and two-stage convolution [24]. This line of efforts motivate our work to develop an efficient and powerful architecture.

Our **contributions**: (i) We propose a new efficient and powerful architectural block, ANTBLOCK, that dynamically utilizes channel relationships; (ii) we show that a naive adaptation of channel attention (e.g., SE) does not improve the representational power of depthwise convolutional layers and propose an optimal configuration that maximizes the number of channels and has *full channel receptive fields*; (iii) using group convolution we make the ANTBLOCK more efficient w.r.t. parameter counts and computational costs without significant performance loss and extend it to an ensemble block; (iv) ANTBLOCK is simple to implement in widely-used deep learning frameworks and outperforms the state-of-the-art lightweight CNNs. ANTNet achieves 0.8% improvement over MobileNetV2 on the ImageNet [19] with 6% fewer parameters and 10% fewer multiply-adds (MAdds) resulting in 20% faster inference time on a mobile phone.

2. Related Work

The efficiency of neural networks becomes an important topic as networks get larger and deeper. Inception module was utilized in GoogLeNet [23] to obtain high performance with a drastically reduced number of parameters by using small convolutions. An efficient bottleneck structure was designed to construct ResNet to achieve high performance. Further, the large demand for on-device applications encourages studies on resource-efficient models with minimal latency and memory usage. To this end, [4] studied module designs with the trade-off between multiple factors such as depth, width, filter size, pooling layer and so on.

Group convolution is a straightforward and effective technique to save computations while maintaining accuracy. It was introduced with AlexNet [16] as a workaround for small GPUs. Later DeepRoots [11] and ResNeXt [25] adopted group convolutions to improve models. Depthwise separable convolution is an extreme case of group convolution that performs convolution each channel separately. It was first introduced in [21] and Xception [2] integrates the idea into the Inception and CondenseNet [9] does so for DenseNet. For mobile platforms, MobileNetV1 [6], and MobileNetV2 [20] used depthwise convolutions with some

hyperparameters to control the size of models.

Channel relationship is a relatively underexplored source of the performance boost. It is a promising direction since it usually requires a small additional cost. ShuffleNets [27, 18] shuffle channels within two-stage group convolution and can be efficiently implemented by ‘‘random sparse convolution’’ layer [1, 26]. Apart from random sparse channel grouping, Squeeze-and-Excitation Networks (SENet) [8] studies a dynamic channel reweighting scheme to boost model capacity at a small cost. The success of channel grouping and channel manipulation motivates our work.

3. Model Architecture: ANTNet

The goal of this work is to design a basic low cost architecture block, which can be used to build efficient Convolutional Neural Networks for mobile devices with budget constraints. The budget of a model varies depending on implementations and hardware quantities for real-world applications. To have a general and fair comparison, in the literature [3], the budget (or complexity) of a model is measured by the number of computations, e.g., multiply-adds (MAdds) or floating point operations (FLOPs), and the number of model parameters. Our goal is to build a more accurate CNN, ANTNet (Attention NesTed Network), with fewer *MAdds* and *Params* by stacking our novel basic blocks. ANTNet utilizes depthwise separable convolution and channel attention. Before introducing our ANTBLOCK, we briefly discuss depthwise separable convolution and its variations with computation budgets (i.e., MAdds, and Params).

Depthwise Separable Convolution is proven to be an effective module to build efficient neural network architectures. It approximates a standard convolution operation with two separate convolutions: depthwise convolution and pointwise convolution. The most common depthwise separable convolution [6] consists of two layers: a 3×3 depthwise convolution that filters the data and 1×1 pointwise convolution that combines the outputs of depthwise convolution. Consider that the input and output of the depthwise separable convolution are three dimensional feature maps of size $H_1 \times W_1 \times C_1$, $H_2 \times W_2 \times C_2$, where H_i , W_i , and C_i denote height, width, and the number of channels of the feature map and i indicates input ($i = 1$) and output ($i = 2$). H_1, H_2 are the height, W_1, W_2 are width, and C_1, C_2 are the number of channels of the input and output feature map. For a convolution kernel size $K \times K$, The total number of MAdds for depthwise separable convolution is

$$(K \times K + C_2) \times C_1 \times H_2 \times W_2. \quad (1)$$

Compared to the standard convolution, it reduces almost $K \times K$ times computational cost. However, it often leads to reduced representational power.

Layer	Input	Operator	Output
(a) Expansion layer	$H \times W \times C_1$	1x1 conv2d, ReLU6	$H \times W \times (C_1 \times t)$
(b) Depthwise layer	$H \times W \times (C_1 \times t)$	3x3 dwise stride = s , ReLU6	$H/s \times W/s \times (C_1 \times t)$
(c) Channel attention layer	$H \times W \times (C_1 \times t)$	Global pooling, FC(2), Sigmoid	$H/s \times W/s \times (C_1 \times t)$
(d) Group-wise projection layer	$H/s \times W/s \times (C_1 \times t)$	linear 1x1 gconv2d group = g	$H/s \times W/s \times C_2$

Table 1: The structure of ANTBlock that it transforms from C_1 to C_2 channels with expansion factor t , group g with stride s .

Inverted Residual Block. One quick fix for the reduced representational power is to increase the input channels for depthwise separable convolution by adding an expansion layer before depthwise convolution in inverted residual bottleneck blocks of MobileNetV2 [20]. The expansion operation expands the number of input channels to t times by 1×1 point-wise convolution. The inverted residual block has three different types of layers, expansion layer, depthwise layer and projection layer. The projection layer takes the largest portion of computation and more parameters than others when the number of input/output channels C is larger than kernel parameters $K \times K$.

Based on our observation on MAdds and parameters of inverted residual block, we will develop a more accurate and efficient block by saving computations on the projection layer with cheaper operations and allocating more resource on the depthwise layer with a small additional cost.

3.1. Designing Efficient Blocks: ANTBlock

In this section, we introduce our ANTBlock with detailed discussion. The ANTBlock presented in Fig. 1(b) is a residual block and can be written as

$$\tilde{\mathbf{x}} = \mathbf{x} + F(\mathbf{x}). \quad (2)$$

When the dimension of the input to the block is not the same as the output, i.e., $(\dim(\mathbf{x}) \neq \dim(\tilde{\mathbf{x}}))$, we simply skip the residual connection as MobileNet V2. For simplicity, let us focus on the equation 2. ANTBlock is motivated by the Inverted Residual Block in MobileNet V2 and it can be factored into two parts: mapping $G(\cdot)$ from the input space to the high dimensional depthwise convolution space, $\mathbf{R}^{H \times W \times tC}$, and projection $H(\cdot)$ to the input space, $\mathbf{R}^{H \times W \times C}$. Then, Eq. 2 can be written as

$$F(\mathbf{x}) = H(G(\mathbf{x})). \quad (3)$$

In ANTBlock, $G(\cdot)$ consists of one expansion layer and one depthwise convolutional layer. $H(\cdot)$ is a projection layer. Now, our block can be rewritten as

$$\tilde{\mathbf{x}} = \mathbf{x} + H(G(\mathbf{x})) \quad (4)$$

This construction can be further improved by the attention mechanism. In [17], the models equipped with attention mask $M(\mathbf{x})$ show significant improvement on segmentation.

We apply this similar idea to the output of depthwise layer for boosting feature representation. In this case, channel attention is used to improve representational power without a significant increase in computational cost and parameters. With channel attention, we can write our ANTBlock (see Fig. 1 (b)) as,

$$\tilde{\mathbf{x}}_c = \mathbf{x}_c + H_c(M(G(\mathbf{x})) * G(\mathbf{x})), \forall c \in \{1, \dots, C\}, \quad (5)$$

where $*$ stands for element-wise product, \mathbf{x} is the input feature, corresponding to the input of ANTBlock in Fig. 1 (b). $G(\mathbf{x})$ denotes the output of depthwise convolution layer (b) of ANTBlock. $M(G(\mathbf{x}))$ denotes the attention mask for $G(\mathbf{x})$, represented by (c)-1, (c)-2 and (c)-3 in Fig. 1 (b). c denotes an output channel of ANTBlock, H_c is the projection for each output channel, corresponding to (d) Fig. 1 (b) with group convolution (group $g = 1$), which means the output of ANTBlock is using all features from the output of attention maps $M(G(\mathbf{x})) * G(\mathbf{x})$.

As discussed before, the parameters and MAdds of depthwise convolutional layer kernels are usually fewer than expansion layer and projection layer. We use a group convolutional layer forward more efficient projection saving parameters and MAdds by a factor of groups. Group convolution first has been adopted in [16] to use multiple GPUs for distributed convolution computation. It reduces computational cost and the number of parameters while still achieving high representational power. [28] proposed *channel local convolution* (CLC), in which an output channel can depend on an arbitrary subset of the input channels. It is a multi-stage group convolution with a nice property so-call *full channel receptive field* (FCRF). They found that in order to achieve high accuracy every output channel of (CLC) should cover all the input channels. In our case, channel attention uses all the input channels of the depthwise convolution layer. So any group convolution for the projection layer satisfies FCRF condition and our ANTBlock becomes a CLC block. With a group convolution layer for the projection layer $H(\cdot)$, our ANTBlock can be written as

$$\tilde{\mathbf{x}}_c = \mathbf{x}_c + H_c(M_{t+1 \dots t + \frac{c'}{g}}(G(\mathbf{x})) * G_{t+1, \dots, t + \frac{c'}{g}}(\mathbf{x})), \quad (6)$$

$$\forall c \in \{1, \dots, C\},$$

where g is the number of group convolution, C' denotes the output channels of $G(\mathbf{x})$, $t = c \pmod{g} \times \frac{c'}{g}$,

$M_{t+1 \dots t+\frac{c'}{g}}(G(\mathbf{x})) * G_{t+1, \dots, t+\frac{c'}{g}}(\mathbf{x})$ denotes the $\frac{c'}{g}$ feature maps associated with each output channel c of ANTBlock. H_c is the projection for each output channel with group convolution (group g), corresponding to (d) Fig. 1 (b).

3.2. Ensemble ANTBlocks: e-ANTBlock

The proposed block (ANTBlock) can be extended further to an ensemble block, denoted by e-ANTBlock. To

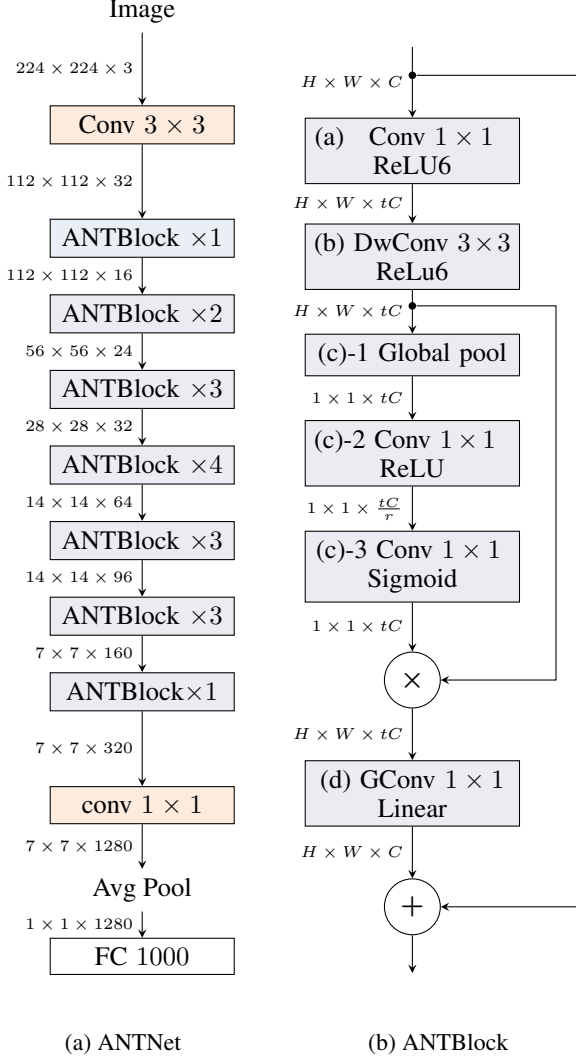


Figure 1: ANTNet architecture for ImageNet. $H \times W \times C$ is the dimension of the tensor, t is the expansion factor of channels, r is the reduction ratio for channel attention. Symbol \oplus denotes the element-wise addition and symbol \otimes denotes the channel-wise multiplication. ANTBlock $\times 1/2/3/4$ means the number of repeated layers within ANTBlock. Note that If the output resolution differs from the input resolution, only the stride of the first layer within ANTBlock is = 2 and residual connection of the block is skipped. DwConv stands for depthwise convolution and GConv stands for group convolution. (a): ANTNet model is shown in Table 2 with more details; (b) is the structure of corresponding ANTBlock for building ANTNet and it is shown in Table 1.

construct more powerful networks, we can ensemble (or weighted aggregate) different types of ANTBlocks (e.g., different group). e-ANTBlock can be written as

$$\tilde{\mathbf{x}} = \mathbf{x} + \sum_{j=1}^m w_j F_j(\mathbf{x}) \quad (7)$$

where m is the number of different ANTBlocks, F_j denotes an ANTBlock with a group convolutional layer for projection, w_j is a weight of an ANTBlock. The weights $\{w_j\}_{j=1}^m$ are outputs of a softmax function written as

$$w_j = \frac{e^{\lambda_j}}{\sum_{j=1}^m e^{\lambda_j}}, 1 \leq j \leq m. \quad (8)$$

so that $\sum_{j=1}^m w_j = 1$ and $\forall w_j \in [0, 1]$. $\{\lambda_j\}_{j=1}^m$ are parameters of e-ANTBlock trained by backpropagation. During

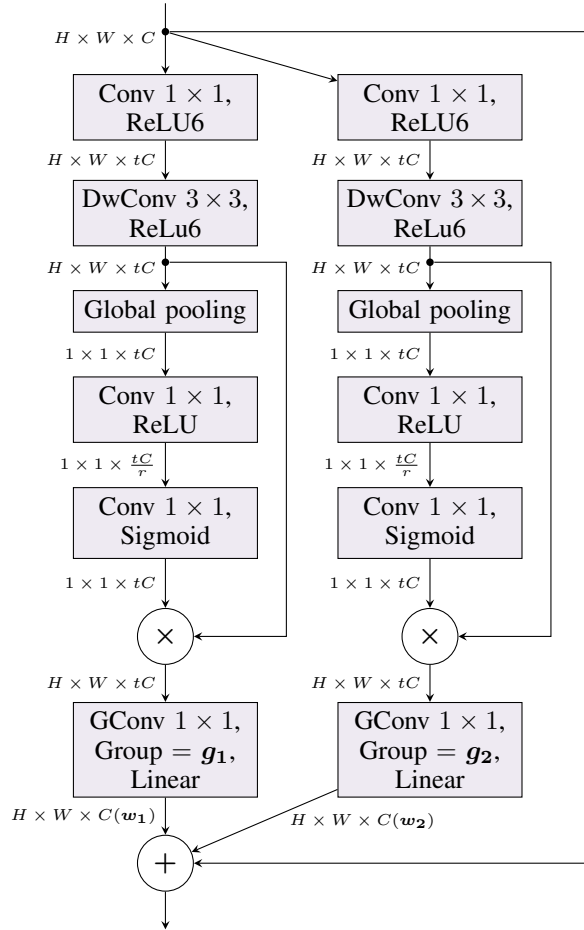


Figure 2: The structure of e-ANTBlock for building e-ANTNet. Two types of ANTBlock are used for constructing e-ANTBlock and the weight parameters w_1 and w_2 of each e-ANTBlock are learned end-to-end for training e-ANTNet built on a sequence of e-ANTBlock. The e-ANTNet architecture is similar to ANTNet except that the ANTBlocks of ANTNet are replaced with e-ANTBlocks.

standard training, these parameters of e-ANTBlock will be learned end-to-end. In our experiments, $j \in \{1, 2\}$ is used. The structure of e-ANTBlock with $m = 2$ can be seen in Fig. 2

3.3. ANTNet

ANTNet (**A**ttention **NesT**ed **N**etwork) is a new efficient convolutional neural network architecture constructed by a sequence of ANTBlocks. The architecture of the network is similar to MobileNetV2, but all the inverted residual blocks are replaced by ANTBlocks and one may use a different number of ANTBlocks depending on the target accuracy.

Now, we describe our architecture in detail. The basic building block is ANTBlock, which has an expansion layer, a depthwise convolutional layer, a channel-attention layer, and a group-wise projection layer with residual connections. The detailed structure of ANTBlock is shown in Table 1 and Figure 1(b).

A channel attention block (c) in Fig.1-(b) introduces additional parameters and MAdds compared to the Inverted Residual Blocks. Consider our ANTNet which has $N = 7$ group of repeated blocks as shown in Table 2. Each group has n_i ANTBlocks. Given reduction ratio r_i , the increase in computational cost can be written as

$$2 * \sum_{i=1}^N n_i \cdot \frac{(C'_i)^2}{r_i}, \quad (9)$$

where C'_i is the number of output channels from the depthwise convolutional layer. The equation 9 shows that when the dimension of output channels increases, the number of additional parameters and MAdds will increase. Also, [7] demonstrates that the channel attention is prone to be saturated at later layers and saturation also appear in our experiments. Therefore, the reduction ratio r_i can be optimized for each repeated blocks and our configuration is shown in Table 2. Later layers have less degree of freedom in terms of channel reweighting.

The group-wise projection layer in the ANTBlock reduces the number of parameters and MAdds. The group parameters g needs to be determined for every ANTBlock for building ANTNet. It is the trade-off between efficiency and model accuracy. The overall design of ANTNet is shown in Table 2. We set the expansion rate $t = 1$ and $g = 1$ for the first repeated blocks (ant0). In others, we use a constant expansion rate and a group throughout the network.

When more budgets (e.g., *MAdds* and *Params*) are allowed, e-ANTBlock can be used as a basic block to build a more powerful network. e-ANTNet achieves the highest accuracy as shown in Table 3.

4. Experiments

We evaluate the computational efficiency and accuracy of ANTNet and compare it with state-of-the-art mobile models with favorable classification accuracy. The computational efficiency is measured theoretically by MAdds, and Params, and empirically by CPU Latency and model size on a mobile platform (iPhone 5s). For accuracy of models, we evaluate the image classification accuracy on CIFAR100 dataset [14] and ImageNet dataset (ILSVRC 2012 image classification) [19]. For ImageNet, we follow the prior work and use the validation dataset as a test set.

ANTNet is implemented using PyTorch. We use built-in 1×1 convolution and group convolution implementation for channel attention, and projection layers. Our ANTBlock is easy to reproduce in any deep learning frameworks such as Caffe, TensorFlow, and MXNet using built-in layers as long as 1×1 standard convolution and group convolution are available.

SGD optimizer was used in our experiments for model training. The momentum of SGD optimizer is set to 0.9 and the *nesterov* momentum is used. We use a multistep learning rate schedule with initial learning rate 0.01 and multiplicative factor of learning rate decay $\gamma = 0.1$ at epoch 200 and 300. The maximum training epoch is set to 400. We set the regularization parameter, *weight decay* during our training process to $4.0e^{-5}$, which is used in the Inception model [23]. The weight decay factor is the same for all the convolution layers in ANTNet. We use the same default data augmentation module as in ResNet for fair comparison. Random cropping and horizontal flipping are used for training images and images are resized or cropped to 224×224 pixels for ImageNet and 32×32 pixels for CIFAR100. During test, the trained model is evaluated on center crops. The same default settings are used in image preprocessing for evaluation as ResNet [5].

4.1. CIFAR100 Classification

The CIFAR100 dataset consists of 32×32 RGB images of 100 classes, with 50,000 training images and 10,000 test images. We consider the start-of-the-art network architecture MobileNetV2 as our baseline. For fair comparison, we keep our settings the same as MobileNetV2. The 32×32 images are converted to 40×40 images with zero-padding by 4 pixels on each side. Then, we randomly sample a 32×32 crop from the 40×40 image. Horizontal flipping and RGB mean value subtraction are applied as well. The overall network architecture and the hyperparameters for CIFAR100 are the same as ANTNet for ImageNet described in Table 2 except for different input and output size (100 classes vs. 1,000 classes) and strides of the first conv2d and the ANTBlock with $14 \times 14 \times 96$ set to 1.

As our purpose is to build resource efficient image classifier on mobile platform, we only compare our model

Name	Input	Operator	Expansion (t)	Reduction Ratio (r)	Output Channels (C_{out})	Repetition (n_i)	Stride (s)	Group (g)
conv0	$224 \times 224 \times 3$	conv2d	-	-	32	1	2	-
ant1	$112 \times 112 \times 32$	ANTBlock	1	8	16	1	1	1
ant2	$112 \times 112 \times 16$	ANTBlock	6	8	24	2	2	2
ant3	$56 \times 56 \times 24$	ANTBlock	6	12	32	3	2	2
ant4	$28 \times 28 \times 32$	ANTBlock	6	16	64	4	2	2
ant5	$14 \times 14 \times 64$	ANTBlock	6	24	96	3	1	2
ant6	$14 \times 14 \times 96$	ANTBlock	6	32	160	3	2	2
ant7	$7 \times 7 \times 160$	ANTBlock	6	64	320	1	1	2
conv8	$7 \times 7 \times 320$	conv2d 1x1	-	-	1280	1	1	-
pool9	$7 \times 7 \times 1280$	avgpool 7x7	-	-	1280	1	1	-
fc10	$1 \times 1 \times 1280$	FC	-	-	n	-	-	-

Table 2: The architecture of ANTNet($g = 2$). Each line gives a sequence of 1 or more identical (modulo stride) layers with repetition times. All layers in the same module or sequence have the same number of output channels. The stride 2 is applied to the only first block in each layer. ANTNet($g = 1$) has the same parameters as above but g is always 1.

with low computational cost models with fewer parameters consuming less memory and taking small network width. We consider mobile-suitable models, MobileNet and ShuffleNet as our comparison baselines. We evaluate the top-1 and top-5 accuracy and compare MAdds and number of parameters for benchmark. The performance comparison between baseline models and our ANTNet is listed in the table 3. It is easy to notice that our ANTNet achieve significant improvements over MobileNetV2 and ShuffleNet with fewer computational cost and parameter count. Our ANTNet ($g = 2$) achieves 19.6% computation reduction and 8.3% parameter reduction with 1.5% increase in top-1 accuracy. Plus, our ANTNet ($g = 1$) achieves more accuracy improvement 1.7% increase of top-1 accuracy with a slightly more computational cost and parameter count.

Network	Top-1 Accu.	Top-5 Accu.	#Parameters	#MAdds
ShuffleNet (1.5)	70.0	90.78	2.3M	91.0M
MobileNetV2	74.2	93.3	2.4M	91.1M
ANTNet ($g = 1$)	75.9	94.3	2.7M	91.4M
ANTNet ($g = 2$)	75.7	93.6	2.2M	73.2M
e-ANTNet	76.7	94.1	4.4M	154.9M

Table 3: Performance on CIFAR100. We compare ANTNet models with MobileNetV2. Our proposed model ANTNet ($g = 2$) achieves 19.6% computation reduction and 8.3% parameter reduction with 1.5% increase in top-1 accuracy.

4.1.1 Optimal Configuration of Channel Attention

Channel attention in the ANTBlock is a key to improve the feature representation but the naive combination of channel attention and Depthwise Separable Convolution does not necessarily yield better performance. Table 4 shows that the naive adaptation of squeeze-and-excitation [8] for MobileNetV2 (Se-MobileNetV2) does not improve the representation power. To combine channel attention with depth-

wise convolutional layers, it needs a more careful design. We observed that channel attention is effective when the number of channels is large. Also similar to Rule for Full Channel Receptive Field (FCRF) [28], we design the ANTBlock that each output channel of a depthwise convolutional layer has a full channel receptive field to maximize the representation power. So, channel attention is inserted between expansion and projection layers in the ANTBlock as proposed in Fig.1 (b). One additional advantage of this design is that since any output channel of the depthwise convolutional layer has a FCRF, the projection layer in the ANTBlock can be substituted with any group convolutional layers ensuring that all output channels of an ANTBlock have a FCRF. All ANTBlocks ($g = 1/g = 2$) have FCRF.

Network	Top-1 Accu.	Top-5 Accu.
MobileNetV2	74.2	93.3
se-MobileNetV2	74.1	92.8
c-ANTNet	73.4	93.3
ANTNet-c	74.4	93.5
ANTNet (proposed)	75.7	93.6

Table 4: Different configurations of channel attention in the ANTBlock are evaluated on CIFAR100. For projection, all ANTNet use group convolution ($g = 2$) and MobileNetV2 uses the standard convolution ($g = 1$). All the blocks have similar computational cost and parameters. Our construction (ANTNet) with channel attention between the depthwise convolution layer and projection layer shows the largest improvement (1.5%). It is consistent with our intuition. Note that a naive adaptation of Squeeze-and-excitation does *not* improve the performance of MobileNetV2. se-MobileNetV2, which has a simple concatenation of a MobileNetV2 block and a SE-Block, shows degradation compared to MobileNetV2. Even in a mobileNetV2 block, channel attention at arbitrary layers such as before the expansion layer (c-ANTNet) and after the projection layer (ANTNet-c) are not effective.

We compare the accuracy of three different arrangements of channel attention against the MobileNetV2 and they have similar computational costs and parameter counts. Our

experiments in Table 4 show that ANTBlock with channel attention between expansion and projection layers was most effective (+1.5% Top-1 Accuracy) whereas all other arrangements do not show a significant performance boost. The channel attention after the projection layer (ANTNet-c) has almost the same performance as MobileNetV2 and channel attention before the expansion layer (c-ANTNet) even reduces the representational power. This experimental result is consistent with our observation and shows that channel attention is most effective with a large number of channels and a full channel receptive field.

4.1.2 Reduction Ratio

Reduction ratios r_i , $i = 1, \dots, N$, in Eq. (9) are hyperparameters to adjust the capacity and MAdds/Params. We varied r_i at each ANTBlock and our final model (ANTNet) achieved the better accuracy (see Table 5) with less parameters rather than fixed r_i for all ANTBlocks. We also observed that the last stage of the network shows an interesting tendency towards a saturated state. We found that the setting of reduction ratio for our ANTNet (see Table 2) achieved a good balance between accuracy and complexity and we thus use this setting for all experiments.

4.1.3 Parameters Learning of e-ANTBlock

Adaptively weighting different types of ANTBlocks, e-ANTBlock, allows building larger models with higher accuracy. In our experiment, we use $m = 2$ types of ANTBlocks (varying number of groups in convolution) by constructing e-ANTBlock. $j \in \{1, 2\}$ indicates we are using two types of ANTBlocks with group convolution with group $g_1 = 1$ and group $g_2 = 2$. w_1 and w_2 are the parameters corresponding to their weights of two types of ANTBlocks. We compared the accuracy on CIFAR100 with manually set weight parameters (w_1, w_2) , e.g., (0,1), (1,0), (0.5,0.5), etc. If we set $w_1 = 1, w_2 = 0$, or $w_1 = 0, w_2 = 1$, it means we are using only one type of ANTBlock for constructing e-ANTBlock and another one type of ANTBlock is not used. When we set $w_1 = 0.5, w_2 = 0.5$, it means we are using both type of blocks for constructing e-ANTBlock by averaging. The experiment on CIFAR100 with e-ANTNet shows that automatic learning w_g outperforms manually setting (see Table

Table 5: Performance comparison of our ANTNet with the configuration of using different reduction ratios r_i for each ANTBlock and fixed r_i for all ANTBlocks on CIFAR100.

Ratio r_i	Params	MAdds	Top-1 accu	Top-5 accu
8	3.5M	92.3M	75.9	94.1
16	3.0M	91.7M	75.2	93.9
32	2.8M	91.5M	75.5	93.9
Ours (mixed)	2.7M	91.4M	75.9	94.3

Table 6: Performance of e-ANTNet with e-ANTBlocks by adaptively weighting two types of ANTBlock on CIFAR100 w/o learning parameters w_1 and w_2 .

w_1	w_2	Top-1 accu
0	1	75.7
1	0	75.9
0.5	0.5	76.2
learned	learned	76.7

6). The best Top1-Accuracy by fixed weights was 76.2% whereas learned (w_1, w_2) achieved 76.7%.

4.2. ImageNet Classification

The ImageNet 2012 dataset consists of 1.28 million training images and 50K validation images from 1,000 classes. We train our network on the training set and report top-1 and top-5 accuracy with the corresponding MAdds and the parameters of models.

Our ANTNet achitecture is shown in Fig 1(a) and the details of layers are listed in the Table 2. We compare our models with other low-cost models (e.g., 3.4 M params, < 300M MAdds), such as MobileNetV1, MobileNetV2 ($\alpha = 1$), and ShuffleNet (1.5). The comparison of accuracy and computation budgets is shown in Table 7. Our ANTNet ($g = 2$) achieves consistent improvement over MobileNetV2 by 0.8% Top-1 accuracy and outperforms ShuffleNet (1.5) by 1.3%. Compared with the most resource-efficient model, CondenseNet ($G=C=4$), our ANTNet performs better than it with 1.8% accuracy improvement, even with fewer MACCs. With slight more parameters and MACCs, our ANTNet ($g = 1$) can offer 1.2% Top-1 accuracy improvement against MobileNetV2 ($\alpha = 1$). Also, we have a variant of our ANTNet which has comparable performance as MobileNetV2 with similar MAdds and Params as CondenseNet ($G=C=4$).

4.3. Inference on a Mobile Device

We briefly discussed that MAdds and Params are used to measure the computational cost and model size. They are handy to compare models across a variety of implementation and hardware. But this estimate does not consider memory reads and writes cost, which can be a crucial factor in a real world scenario. Since memory access is relatively slower than computations, the amount of memory access will have a big impact on its real speed on actual devices. Moreover, both CPUs and GPUs can do caching to speed up memory reads and writes. Memory coalescing can be very useful for speeding up memory reads as each thread can read a chunk of memory in one go instead of doing separate reads. Kernels can also read small amounts of memory into local or thread group storage of faster access. It is possible for each thread to compute multiple outputs instead of only one, allowing it to reuse some of the input multiple

Model	#Parameters	#MAdds	Top-1 Accu. (%)	Top-5 Accu. (%)
MobileNetV1	4.2M	575M	70.6	89.5
SqueezeNext	3.2M	708M	67.5	88.2
ShuffleNet (1.5)	3.4M	292M	71.5	-
ShuffleNet (x2)	5.4M	524M	73.7	-
CondenseNet (G=C=4)	2.9M	274M	71.0	90.0
CondenseNet (G=C=8)	4.8M	529M	73.8	91.7
MobileNetV2	3.4M	300M	72.0	91.0
MobileNetV2 (1.4)	6.9M	585M	74.7	92.5
NASNet-A	5.3M	564M	74.0	91.3
AmoebaNet-A	5.1M	555M	74.5	92.0
PNASNet	5.1M	588M	74.2	91.9
DARTS	4.9M	595M	73.1	91
ANTNet (g = 1) (ours)	3.7M	322M	73.2	91.2
ANTNet (g = 2) (ours)	3.2M	267M	72.8	91.0
e-ANTNet (ours)	5.5M	545M	74.2	91.6
ANTNet ($\alpha = 1.4$) (ours)	6.8M	598M	75.0	92.3

Table 7: Performance Results on ImageNet Classification. We compare our AntNet models with mobile models. Our proposed model ANTNet ($g = 2$) achieves 0.8% absolute Top-1 accuracy improvement over MobileNetV2 with 6% fewer parameters and 11% fewer MAdds. Compare with the lightest model CondenseNet (G=C=4), our model achieves 1.8% absolute Top-1 accuracy with fewer MAdds. To compare with $\sim 600M$ #MAdds, we increase the dimension of features with depth multiplier ($\alpha = 1.4$) of our ANTNet, ANTNet ($\alpha = 1.4$), and it performs better than all baseline models, 0.3% Top-1 accuracy improvement over MobileNetV2 (1.4), 1% Top-1 accuracy improvement over NASNet-A and 2% Top-1 accuracy improvement over DARTS.

times and thus requiring fewer memory reads overall. In short, the actual inference speed running on actual devices depends on hardware architecture and the ways of implementation of each layer. So the inference speed of models should be tested on actual devices as well.

We evaluate the actual inference time of models on a commodity iOS-based smartphone *iPhone 5s*, which has a 64-bit 1.3 GHz dual-core Apple Cyclone, Apple A7, Apple M7 motion coprocessor and 1GB LPDDR3 RAM. To run the inference of models on iPhone5s, we need to convert our trained models to *CoreML* models, which can be deployed on iOS-based devices using an Apple machine learning platform. CoreML is optimized for on-device performance and minimizes memory footprint and power consumption. Although it is only focused on and optimized on iOS-based platform, it can still be meaningful to compare the speed of ANTNet relative to other baseline models. The actual inference time of models on iPhone 5s is available in Table 8. We run each model 10 times and take out the fastest and the slowest runs, and then take average of 8 runs as the final

Model	MAdds	CoreML Model Size	Latency
MobileNetV2	300M	14.7M	197.2ms
ANTNet (g = 1)	322M	15.8M	214.2ms
ANTNet (g = 2)	267M	13.4M	157.7ms

Table 8: Latency (inference time) running on an actual device, iPhone 5s. Our proposed model ANTNet ($g = 2$) achieves 20% faster than MobileNetV2.

inference time. The table also provides converted CoreML model file sizes. Table 8 shows that our ANTNet ($g = 2$) achieves 20% speedup compared to MobileNetV2 and the improvement of latency is our analysis of MAdds.

The CPU inference time on a desktop machine with a 2.10 GHz 32-core Intel(R) Xeon(R) CPU E5-2620 shows similar improvement as *iPhone 5s* that our ANTNet ($g = 2$) is 8% faster than MobileNetV2 (1.11s vs 1.21s).

5. Conclusion

In this paper we proposed the ANTBlock, a novel basic architecture unit designed to boost the representational capacity of a network by imposing channel-wise attention and grouped convolution. The capacity of ANTBlock allows designing resource-efficient networks. MobileNetV2 can be viewed as a special case of our network with the removal of channel-wise attention and group convolution. Extensive experiments demonstrate the effectiveness and efficiency of our ANTNet which achieves state-of-the-art performance on multiple datasets. In addition, the experiments on an actual device iPhone 5s show that ANTNet achieves significant latency improvement on top of state-of-the-art low cost models in practice. Finally, the improved capacity induced by ANTBlocks shows that leveraging the interdependency of channels is a promising direction to find more resource-efficient mobile models by imposing MAdds and parameter constraints.

Acknowledgments. We thank Amrith Tyagi, James M. Rehg and Yadunandana Rao for discussions.

References

- [1] Soravit Changpinyo, Mark Sandler, and Andrey Zhmoginov. The power of sparsity in convolutional neural networks. *arXiv preprint arXiv:1702.06257*, 2017.
- [2] François Chollet. Xception: Deep learning with depthwise separable convolutions. *arXiv preprint*, pages 1610–02357, 2017.
- [3] Song Han, Jeff Pool, John Tran, and William Dally. Learning both weights and connections for efficient neural network. In *Advances in neural information processing systems*, pages 1135–1143, 2015.
- [4] Kaiming He and Jian Sun. Convolutional neural networks at constrained time cost. In *Proceedings of the IEEE conference on computer vision and pattern recognition*, pages 5353–5360, 2015.
- [5] Kaiming He, Xiangyu Zhang, Shaoqing Ren, and Jian Sun. Deep residual learning for image recognition. In *Proceedings of the IEEE conference on computer vision and pattern recognition*, pages 770–778, 2016.
- [6] Andrew G Howard, Menglong Zhu, Bo Chen, Dmitry Kalenichenko, Weijun Wang, Tobias Weyand, Marco Andreetto, and Hartwig Adam. Mobilenets: Efficient convolutional neural networks for mobile vision applications. *arXiv preprint arXiv:1704.04861*, 2017.
- [7] Jie Hu, Li Shen, and Gang Sun. Squeeze-and-excitation networks. *arXiv preprint arXiv:1709.01507*, 7, 2017.
- [8] Jie Hu, Li Shen, and Gang Sun. Squeeze-and-excitation networks. 2018.
- [9] Gao Huang, Shichen Liu, Laurens van der Maaten, and Kilian Q. Weinberger. Condensenet: An efficient densenet using learned group convolutions. In *The IEEE Conference on Computer Vision and Pattern Recognition (CVPR)*, June 2018.
- [10] Gao Huang, Zhuang Liu, Laurens Van Der Maaten, and Kilian Q Weinberger. Densely connected convolutional networks. In *CVPR*, volume 1, page 3, 2017.
- [11] Yani Ioannou, Duncan Robertson, Roberto Cipolla, Antonio Criminisi, et al. Deep roots: Improving cnn efficiency with hierarchical filter groups. 2017.
- [12] Sergey Ioffe and Christian Szegedy. Batch normalization: Accelerating deep network training by reducing internal covariate shift. *arXiv preprint arXiv:1502.03167*, 2015.
- [13] Jonghoon Jin, Aysegül Dundar, and Eugenio Culurciello. Flattened convolutional neural networks for feedforward acceleration. *arXiv preprint arXiv:1412.5474*, 2014.
- [14] Alex Krizhevsky. Learning multiple layers of features from tiny images. Technical report, Citeseer, 2009.
- [15] Alex Krizhevsky, Ilya Sutskever, and Geoffrey E Hinton. Imagenet classification with deep convolutional neural networks. In F. Pereira, C. J. C. Burges, L. Bottou, and K. Q. Weinberger, editors, *Advances in Neural Information Processing Systems 25*, pages 1097–1105. Curran Associates, Inc., 2012.
- [16] Alex Krizhevsky, Ilya Sutskever, and Geoffrey E Hinton. Imagenet classification with deep convolutional neural networks. In *Advances in neural information processing systems*, pages 1097–1105, 2012.
- [17] Jonathan Long, Evan Shelhamer, and Trevor Darrell. Fully convolutional networks for semantic segmentation. In *Proceedings of the IEEE conference on computer vision and pattern recognition*, pages 3431–3440, 2015.
- [18] Ningning Ma, Xiangyu Zhang, Hai-Tao Zheng, and Jian Sun. Shufflenet v2: Practical guidelines for efficient cnn architecture design. *arXiv preprint arXiv:1807.11164*, 2018.
- [19] Olga Russakovsky, Jia Deng, Hao Su, Jonathan Krause, Sanjeev Satheesh, Sean Ma, Zhiheng Huang, Andrej Karpathy, Aditya Khosla, Michael Bernstein, et al. Imagenet large scale visual recognition challenge. *International Journal of Computer Vision*, 115(3):211–252, 2015.
- [20] Mark Sandler, Andrew Howard, Menglong Zhu, Andrey Zhmoginov, and Liang-Chieh Chen. Mobilenetv2: Inverted residuals and linear bottlenecks. In *Proceedings of the IEEE Conference on Computer Vision and Pattern Recognition*, pages 4510–4520, 2018.
- [21] Laurent Sifre and Stéphane Mallat. *Rigid-motion scattering for image classification*. PhD thesis, Citeseer, 2014.
- [22] Rupesh K Srivastava, Klaus Greff, and Jürgen Schmidhuber. Training very deep networks. In *Advances in neural information processing systems*, pages 2377–2385, 2015.
- [23] Christian Szegedy, Wei Liu, Yangqing Jia, Pierre Sermanet, Scott Reed, Dragomir Anguelov, Dumitru Erhan, Vincent Vanhoucke, and Andrew Rabinovich. Going deeper with convolutions. In *Proceedings of the IEEE conference on computer vision and pattern recognition*, pages 1–9, 2015.
- [24] Guotian Xie, Jingdong Wang, Ting Zhang, Jianhuang Lai, Richang Hong, and Guo-Jun Qi. Interleaved structured sparse convolutional neural networks. In *Proceedings of the IEEE Conference on Computer Vision and Pattern Recognition*, pages 8847–8856, 2018.
- [25] Saining Xie, Ross Girshick, Piotr Dollár, Zhuowen Tu, and Kaiming He. Aggregated residual transformations for deep neural networks. In *Computer Vision and Pattern Recognition (CVPR), 2017 IEEE Conference on*, pages 5987–5995. IEEE, 2017.
- [26] Ting Zhang, Guo-Jun Qi, Bin Xiao, and Jingdong Wang. Interleaved group convolutions. In *Computer Vision and Pattern Recognition*, 2017.
- [27] Xiangyu Zhang, Xinyu Zhou, Mengxiao Lin, and Jian Sun. Shufflenet: An extremely efficient convolutional neural network for mobile devices. In *The IEEE Conference on Computer Vision and Pattern Recognition (CVPR)*, June 2018.
- [28] Dong-Qing Zhang et al. clcnet: Improving the efficiency of convolutional neural network using channel local convolutions. *arXiv preprint arXiv:1712.06145*, 2017.